A novel extension to non-local means algorithm: application to brain MRI de-noising

[a]Muhammad Aksam Iftikhar, [b]Saima Rathore, [c]Abdul Jalil, [d]Mutawarra Hussain,
DCIS, Pakistan Institute of Engineering and Applied Sciences, Islamabad, Pakistan
[a]aksam.iftikhar@gmail.com, [b]saimarathore_2k6@yahoo.com, [c]jalil@pieas.edu.pk, [d]mutawarra@pieas.edu.pk

***Abstract*—Image de-noising is an essential intermediate step in several medical applications related to brain MRI. The noise present in brain MRI degrades the performance of computer-aided analysis of these images. Therefore, the noise should be removed prior to subsequent processing. Non-local means (NLM) is a classical de-noising algorithm, which has been successfully applied for de-noising of brain MRI. In this work, a variant of traditional NLM, called improved adaptive non-local means (IANLM), has been extended for application to brain MRI. The new algorithm is named as extended non-local means (ExNLM) algorithm. To be precise, the IANLM algorithm is adapted to Rician noise inherently present in MR images by using a Ricain bias correction procedure. Moreover, a wavelet coefficient mixing procedure is proposed which exploits valuable information in different sub bands of over- and under-smoothed images, obtained by using the IANLM algorithm with different set of parameters. Finally, optimization of the proposed ExNLM algorithm is performed for brain MR images de-noising. Different variants of the proposed algorithm have been validated on a simulated brain MRI dataset. Quantitative and qualitative results indicate that the proposed algorithm suppresses the noise in brain MR images effectively, and outperforms several contemporary methods of de-noising.**

***Keywords*—non-local, de-noising, MRI, Rician, wavelet mixing**

I. Introduction

Brain MRI is a popular tool, which is used by clinical experts to diagnose various diseases and disorders of brain like Alzheimer's disease, multiple sclerosis, Parkinson's disease etc. Brain MR images are usually affected by artifacts and thermal noise due to the limitations associated with the equipment used for imaging. The noise severely degrades the quality of MR images and affects further quantitative assessment from the data. Therefore, it is desirable to remove noise from these images – a process referred to as image de-noising.

Many de-noising methods use the principle of averaging similar voxels of input MR image in order to obtain restored value of the voxel under consideration. However, other techniques also exist which exploit statistical characteristics of local neighborhood of a voxel [1]. Gaussian filtering has also been used for de-noising [2]; however, it results in over-smoothing of the input image. The over-smoothed image loses most of the edge information and fine detail in the underlying noise-free image. Diffusion filtering provides a suitable alternate for edge preservation in the de-noising process [3-5]. However, these filters enhance the image in an unnatural way and remove small features in the image. Wavelet filtering has been used for de-noising purpose as noisy content can be separated from the original signal by a suitable thresholding method in the wavelet domain [6, 7]. However, these filters also introduce characteristic artifacts, which may severely degrade the quality of restored image.

A patch based non-local means (NLM) [8] filter has been proposed by in order to cope with most of the aforesaid limitations. The patch of a pixel refers to the set of pixels in a local neighborhood of the pixel. In order to restore the value of a pixel, the NLM filter computes weighted average of pixels within a search window. The weights are computed by measuring the similarity of patch of current pixel with that of pixels in the search window. The search window was assumed to be the whole image in the originally proposed NLM filter [8]; however, this assumption severely penalizes the algorithm computationally. Therefore, in later implementations, the search area is limited to a window of particular size [9, 10]. This produces a computationally tractable NLM filtering without much compromising its de-noising effectiveness. The computational efficiency as well as the de-noising performance of NLM was further improved by an adaptive search window based variant of NLM [11]. This variant, named as improved adaptive NLM (IANLM), introduces an adaptive search window for each pixel based on a weight threshold. The weight threshold is used to determine the set of sufficient number of suitable pixels for participation in the de-noising process. As soon as a set of sufficient number of suitable pixels (determined empirically) is available, the search process is truncated, thereby resulting in an adaptive search window.

The NLM algorithm has also been adapted specifically to the type of noise present in MR images [10, 12]. The noise in MRI follows Rician distribution, which is known to introduce certain bias for image regions having different overall intensities. Such bias has been removed with a bias correction method that filters squared input magnitude MR image rather than the image itself [13]. The UNLM (unbiased non-local means) filter proposed in [10] follows this approach to yield much improved restoration of noisy brain MR images.

Different variants of NLM have also been proposed for 3D brain MRI de-noising. An optimized non-local means filter for brain MRI de-noising has been proposed in [9], which combines the 3D implementation of traditional NLM with concepts such as voxel pre-selection, automatic parameter tuning and Rician bias correction. Vega et al. proposed

comparing truncated local Taylor series based descriptive features of patches rather than comparing intensity values of patches [14]. This approach has inherent computational advantage, as in most cases, the features of patches are substantially lower in number than original intensity values. Similarly, a wavelet sub-band mixing procedure has been proposed in [15] for 3D brain MRI de-noising, which combines different sub-bands of over- and under-smoothed images obtained by using NLM filter with different parameters. The concept of wavelet mixing has been further extended in [16], wherein the filter has been adapted to the amount of noise by using adaptive soft wavelet mixing based on frequency and spatial information in the image.

In this work, we have extended the IANLM algorithm proposed in [11], and the new algorithm is named as extended non-local means (ExNLM). The ExNLM algorithm incorporates following extensions to the IANLM filter. First, IANLM is a variant of traditional NLM and does not take into account the special nature of MR images. In ExNLM, we have adapted the IANLM algorithm to Rician noise, similar to the way NLM has been adapted in [10]. Second, a wavelet mixing procedure is proposed in order to exploit valuable information from different sub-bands of the over- and under-images obtained by using IANLM algorithm with different set of parameters. Finally, the proposed algorithm is optimized for application to brain MR images. Different variants of ExNLM have been presented in order to investigate the influence of individual extensions proposed in this work. These variants have been validated on simulated brain MRI and compared with other state of the art methods in de-noising. Improved quantitative and qualitative results using ExNLM show the superiority of the proposed algorithm over contemporary methods.

Rest of the paper is organized as follows. Section II describes the proposed methodology in detail. Experimental setup is described in Section III, while detailed results of experiments are presented in Section IV. Finally, the research work is concluded and prospective future directions are set in Section V.

II. Proposed Methodology

The proposed ExNLM algorithm is characterized by following major components.

1. IANLM filtering (see Section II (A)).
2. Rician noise correction (see Section II (B)).
3. Wavelet coefficient mixing (see Section II (C)).
4. Paramters optimization (see Section II (D)).

The above steps should be followed in the specified sequence to obtain ExNLM-filtered image. Note that the parameters optimization procedure should be applied only once for a particular type of application (brain MRI de-noising in our case) .

A. IANLM

The traditional non-local means computes similarity weights among pixels within a search window. The search window is traversed exhaustively in order to compare patches of pixels in the window with the central patch corresponding to current pixel. The de-noising process in NLM can be formulated as follows.

$$x_i = \sum_{j \in S_i} w_{ij} y_j, \quad \textit{subject to} \sum_{j \in S_i} w_{ij} = 1 \tag{1}$$

Where y_j represents the j_{th} noisy pixel in the set of pixels (S_i) within the search window of pixel i, and x_i represents the NLM-restored value of pixel i. The similarity weight (w_{ij}) between patches $\boldsymbol{P_i}$ (patch of pixel i is referred as $\boldsymbol{P_i}$ in the following text) and $\boldsymbol{P_j}$ is computed using the following expression:

$$w_{ij} = \frac{1}{Z_i} e^{-\frac{\left(\| y(P_i) - y(P_j) \|_2^2\right)}{h^2}} \tag{2}$$

Where h is the smoothing factor which controls the tradeoff between smoothness (noise removal) and detail preservation. $\|\boldsymbol{y(P_i)-y(P_j)}\|_2$ denotes the Euclidian distance between patches $\boldsymbol{P_i}$ and $\boldsymbol{P_j}$, where $\boldsymbol{y(P_i)}$ and $\boldsymbol{y(P_j)}$ are the intensity values of pixels in Patch $\boldsymbol{P_i}$ and $\boldsymbol{P_j}$, respectively. The term Z_i is a normalization constant which makes sure that $w_{ij} \in [0,1]$.

The exhaustive search process within the search window poses severe computational burden without significant performance advantage. As mentioned earlier in Section I, IANLM [11] is a variant of NLM, which presents an adaptation mechanism for automatic selection of search window size for a particular pixel. The adaptation mechanism is based on number of *fit* pixels/patches found within particular search window. A fit pixel corresponds to a pixel for which the similarity weight is greater than a particular threshold. Hence, IANLM can be mathematically formulated as follows.

$$x_i^{'} = \sum_{j \in N_i^*} w_{ij} y_j, \quad \textit{subject to} \sum_{j \in N_i^*} w_{ij} = 1 \tag{3}$$

Where x_i' is the IANLM-restored value for pixel i and $N_i^* \subseteq S_i$ is the set of pixels around pixel i, satisfying following constraints.

- Robust threshold criterion: $w_{ij} > w_\theta$, where w_θ is a threshold on similarity between pixels i and j.
- Window adaptation test: $|N_i^*| \leq N_f$, where N_f is the number of fit pixels' within the search window.

B. Rician Correction

The noise contained in MR images follows Rician distribution [17]. The Rician noise is characterized by biased behavior for different regions of the image. The low and high intensity regions are affected differently by Rician noise, due to which overall contrast of the image is reduced. However, this bias can be annulled effectively by filtering the squared magnitude image rather than the image itself and subtracting the amount of bias from restored value of each pixel [13]. The amount of bias is double the noise variance for MR images. Therefore, the said Ricain bias correction method can be formulated as follows.

$$x_i'' = \sqrt{x_i' - 2\sigma^2} \tag{4}$$

Where x_i' is the restored value of pixel i by IANLM algorithm, and x_i'' is the unbiased restored value obtained after applying the bias correction.

C. Wavelet Coefficients Mixing

Wavelet filtering is a classical tool for noise suppression in images. The traditional approach in wavelet domain de-noising is to suppress coefficients of different sub-bands beyond a certain threshold. Two methods of thresholding are in practice, namely hard and soft wavelet threshold. The hard thresholding method altogether eliminates the coefficients below a particular threshold. Whereas, the soft threshold considers a more smooth suppression of wavelet coefficients based on the threshold.

In this paper, we have exploited the capability of wavelets, to separate low and high frequency components of the image, for better de-noising. In particular, two versions of the filtered image are obtained by using different filtering parameters in the IANLM algorithm. The two filtered images correspond to over- and under-smoothed images. The over-smoothed image (I_o) removes the noise efficiently but fine image details are lost. On the contrary, the under-smoothed image (I_u) preserve small image structures, however, the noise is not removed to its full potential. We propose to combine different sub-bands of the two images so that positive features of each image are incorporated in the final restored image. The image is decomposed into four sub-bands (1st level) in the wavelet domain, namely approximation (w_a), horizontal detail (w_h), vertical detail (w_v) and diagonal detail (w_d). In this way, the sub-bands corresponding to I_o and I_u are denoted by ($w_{a,u}$, $w_{h,u}$, $w_{v,u}$, $w_{d,u}$) and ($w_{a,o}$, $w_{h,o}$, $w_{v,o}$, $w_{d,o}$), respectively. To obtain the final restored image, soft thresholding is first applied to I_u. Then, the three sub-bands of I_u, namely $w_{h,u}$, $w_{v,u}$ and $w_{d,u}$, are combined with $w_{a,o}$ from I_o. In this way, we effectively exploit the efficient noise removal characteristic of I_o, and detail preservation capability of I_u. The wavelet coefficient mixing procedure is illustrated graphically for a brain MR image in Figure 1. The discrete wavelet transform is used to decompose over- and under-smoothed images into four sub-bands each. The final filtered image is obtained by combining different sub-bands and then applying the soft thresholding and inverse discrete wavelet transform to combined sub-bands. Note that improved PSNR measure is obtained for the final filtered image obtained after applying the mixing procedure.

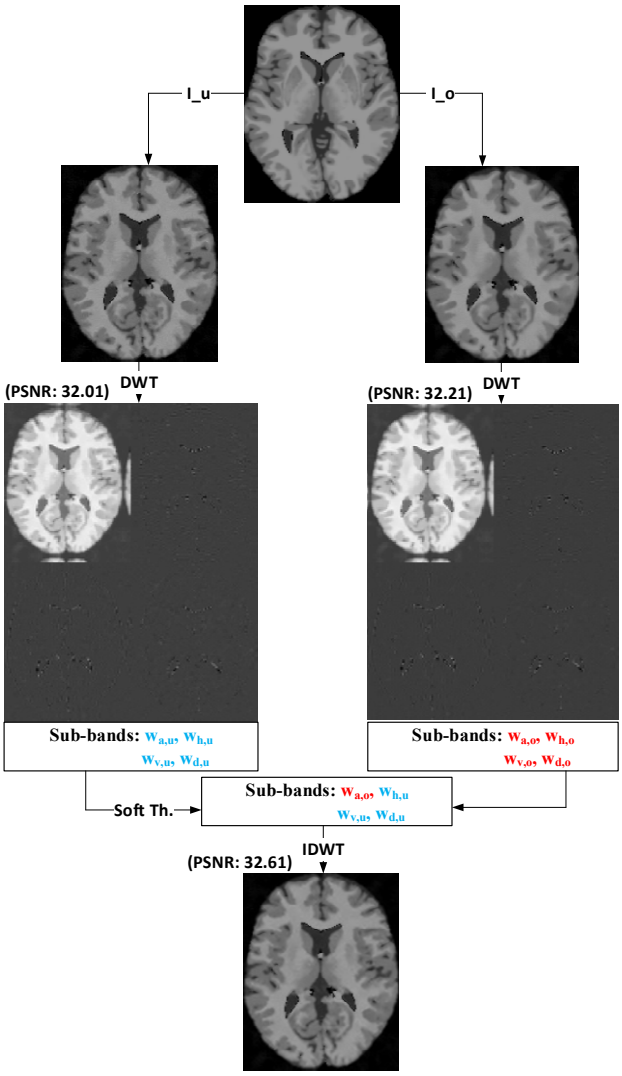

Figure 1: The proposed wavelet coefficient mixing procedure

D. Optimization of ExNLM

The proposed ExNLM algorithm includes several crucial parameters, whose values are critical to the performance of the algorithm. Therefore, optimal values of these parameters should be obtained for a particular application. These parameters are listed as follows.

- p: radius of patch. Patch size = $(2p + 1 \times 2p + 1)$
- s: radius of search window. Search window size = $(2s + 1 \times 2s + 1)$
- w': weight assigned to central pixel/patch in the de-noising process.
- k: relates the smoothing parameter h to σ, as $h = k\sigma$, where σ is standard deviation of noise in input image.
- Nf: Maximum number of fit patches before the search in truncated in current search window.
- $\boldsymbol{w}_{\square}$: Robust threshold on similarity weights.

Optimal values of these parameters for brain MRI de-noising have been obtained as described in Section III (C).

III. Experimental Setup

The proposed ExNLM algorithm has been validated on simulated brain MRI corrupted with Rician noise of various levels. In order to study the individual impact of different extensions to the IANLM algorithm which are proposed in this research, we have considered following variants of the proposed algorithm.

- $ExNLM_1$: Unoptimized IANLM with Rician Correction.
- $ExNLM_2$: Optimized IANLM with Rician Correction.
- ExNLM: Optimized IANLM with Rician Correction and wavelet mixing.

The values of different parameters for $ExNLM_1$ have been inherited from [11]. Whereas, optimization of parameters for other versions of ExNLM algorithm will be presented shortly (see Section III (C)). The said variants of the proposed ExNLM algorithm have been applied to de-noise simulated brain MR images at various noise levels and performance is measured in terms of a well-known performance metric – Peak Signal to Noise Ratio (PSNR). For a particular image, the PSNR is computed against reference image using following expression.

$$\mathrm{PSNR} = 10\log_{10}(R^2 / MSE) = 20\log_{10}(R / RMSE) \qquad (5)$$

Where, R represents the maximum possible intensity value of a pixel in the image. RMSE represents Root Mean Square Error between the filtered and reference (noise-free) image.

A. Data Set

In this work, simulated brain MR data has been used for validation of the proposed ExNLM algorithm. The simulated brain MRI volume is a part of the BrainWeb freely available database (www.bic.mni.mcgill.ca/brainweb/) and has been generated with the help of an MRI simulator. The dimensions of the 3D brain volume are 181x217x181 and slice thickness is 1mm. The simulated brain volume is available in different MRI modalities like T1-weighted, T2-weighted, and proton density (PD) images. We have used T1-weighted MRI data in our experiments.

B. Brain extraction

The MR images available in the simulated brain volume on BrainWeb are complete head MRI, which contain other tissues like skull, fat etc. along with the brain portion. We have extracted the brain portion prior to subsequent experimentation so that irrelevant tissues do not affect the results reported for brain MRI de-noising. Brain extraction is a comprehensive research field on its own; however, we have used ground truth for segmentation of different brain tissues, available with the BrainWeb database, for brain surface extraction. The ground truth has been used as a mask to obtain

(a) (b) (c)

Figure 2: Brain surface extraction, (a) original head MR image, (b) the mask for brain portion and (c) MR image with brain portion only

the cropped image containing the brain portion only. An example of extracting the brain portion from original head MRI is shown in Figure 2. Note that the brain MR image in Figure 2 (c) contains a lot of background area. However, in order to remove any favorable bias of results due to background tissue, this tissue is excluded from any quantitative performance measurement reported in this work.

C. Optimization of ExNLM for brain MRI de-noising

As stated previously, different parameters are critical to the de-noising performance of the proposed ExNLM algorithm. Therefore, we have obtained optimal values of these parameters for application to brain MRI de-noising. To this end, the performance of the algorithm has been tested over appropriate range of values of these parameters and optimal value is selected for each parameter.

The optimal values of two parameters, namely s and p, have been obtained in [10] for classical NLM algorithm to be 5 and 2, respectively. After substantial empirical testing, we have found that these values are suitable for the proposed ExNLM algorithm as well. Similarly, the parameter $w_{\square}$ has been set to 0.01 in [11] for the IANLM algorithm. Similar to s and p, this value of $w_{\square}$ is suitable for the proposed ExNLM algorithm. Optimal selection for rest of the parameters is performed empirically, and is shown in Figure 3. Table I summarizes optimal values of all the parameters, used in this work, for different variants of the proposed algorithm.

TABLE I. OPTIMAL PARAMETER VALUES FOR DIFFERENT EXNLM VARIANTS

Variant	*P*	*S*	*w'*	*k*	*Nf*	$w_{\square}$
$ExNLM_1$	2	5	w_{max}	1.2	27	.01
$ExNLM_2$	2	5	.1	1	50	.01
ExNLM (I_o)	2	5	.1	1	50	.01
ExNLM (I_u)	1	5	.1	.9	50	.01

IV. EXPERIMENTS ON SIMULATED BRAIN MRI

In this section, we have validated different variants of the proposed algorithm on T1-weighted simulated brain MRI. The de-noising performance of different algorithms is analyzed and is compared with other contemporary algorithms both qualitatively and quantitatively. Section IV (A) compares different variants of the proposed algorithm with IANLM and a few other contemporary algorithms. Whereas, qualitative comparison of de-noising results using different algorithms has been performed visually in Section IV (B).

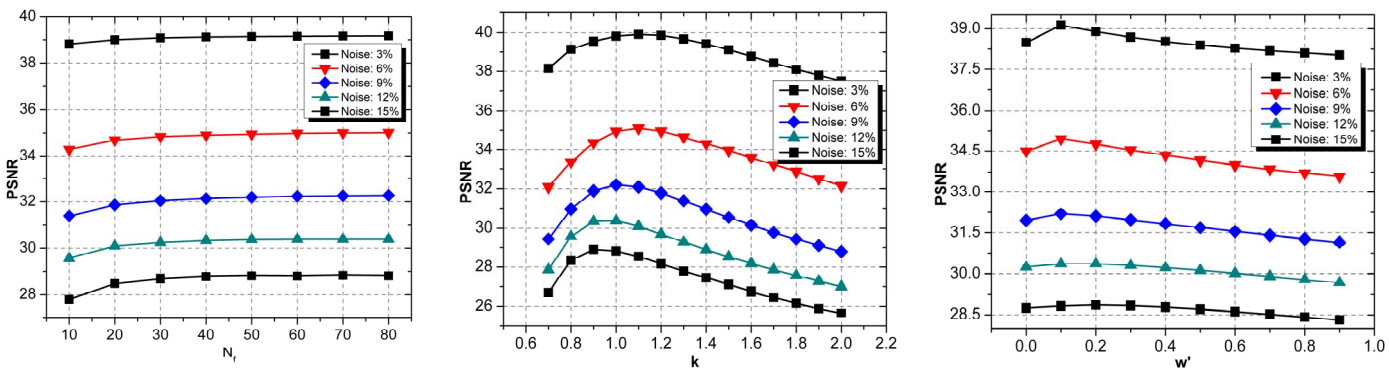

(a) (b) (c)

Figure 3: Optimization of ExNLM algorithm for (a) Maximum number of fit patches (N_f), (b) the scaling parameter (k), (c) weight of central patch (w')

A. Quantitative Analysis

The quantitative performance of different algorithms has been analyzed in two ways. First, different variants of the proposed ExNLM algorithm have been compared with the IANLM algorithm, in order to realize the improvement induced by each proposed extension to IANLM. Second, the ExNLM algorithm (encompassing all extensions to IANLM) has been compared with a few other state of the art de-noising methods including UNLM [10], OWT-SURELET [6] and Bayesian estimation de-noising [18].

1) Influence of proposed extensions to IANLM: Figure 4 graphically shows PNSR measures obtained for different variants of the proposed ExNLM and IANLM algorithm at various noise levels. Clear advatange is evident for all the variants of ExNLM over IANLM algorithm. Also, it can be observed that optimization of the algorithm improves its performance (compare $ExNLM_1$ and $ExNLM_2$) over all noise levels. Similarly, maximum performance is obtained with ExNLM which incorporates all the extensions to the IANLM algorithm proposed in this work. Therefore, we present further results for ExNLM in subsequent text.

2) Comparison with contemporary methods:

We have compared the performance of the proposed algorithm with other contemporary algorithms in two parts. First, the ExNLM algorithm is compared with UNLM in Table II. The UNLM method is an extension of traditional NLM algorithm adapted to Rician bias correction. Therefore, it is more reasonable to compare it seperately with ExNLM. It can be concluded from quantitative results in Table II that the proposed ExNLM algorithm is not only more robust to noise, but is also more reliable among various tests as the standard deviation is less than UNLM at all noise levels.

To obtain more reliable comparison, the proposed ExNLM algorithm has also been compared with two other contemporary de-noising methods. First method minimizes the error between noisy and reference (noise-free) images based on orthogonal wavelet transform [6]. As reference image is not available in many practical applications, the mean square error is estimated using an unbiased estimate of risk, known as Stein's unbiased risk estimate (SURE). Hence, the method is named as (OWT-SURELET). The second method used here for comparison finds a Bayesian approximation of the reference image based on the conditional posterior sampling approach [18].

TABLE II. PERFORMANCE COMPARISON OF UNLM AND EXNLM

Noise (%)	UNLM		ExNLM	
	Avg.	*Std.*	*Avg.*	*Std.*
3	37.79	1.22	**39.40**	**0.59**
6	34.49	1.07	**34.98**	**0.72**
9	31.77	1.07	**32.17**	**0.94**
12	29.76	1.05	**30.12**	**1.00**
15	28.24	1.03	**28.61**	**0.96**

Figure 5 compares PSNR measures at various noise levels for ExNLM, OWT-SURELET and Bayesian estimation de-noising methods. The superiority of ExNLM is clearly visible from large performance margin of the proposed algorithm over other two algorithms.

B. Qualitative Analysis

Qualitative results of various de-noising methods have been compared in this section. A brain MR image, and images obtained by de-noising corresponding noise-corrupted (9%) image are shown in Figure 6. By comparing the quality of restored images visually, it can be observed that the ExNLM-restored image is much close in appearance to the original (noise-free) image. Other methods of de-noising either do not remove noise effectively (see Figure 6 (e) and (f)) or remove small structures from the restored image (see Figure 6 (c) and (d)). Therefore, it can be concluded reasonably that the proposed algorithm outperforms all other de-noising methods.

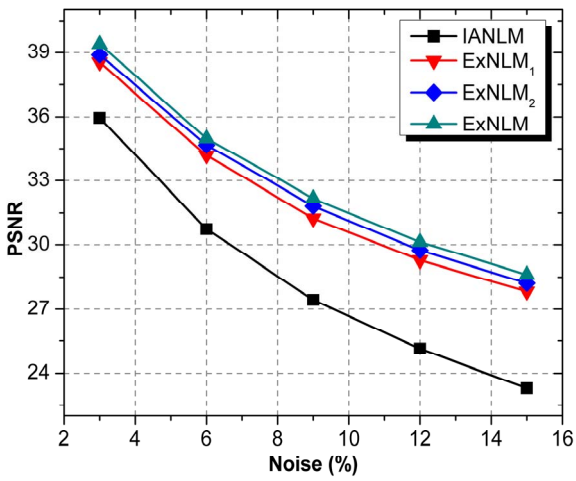

Figure 4: Quantitative comparison of different variants of ExNLM and IANLM in terms of PSNR

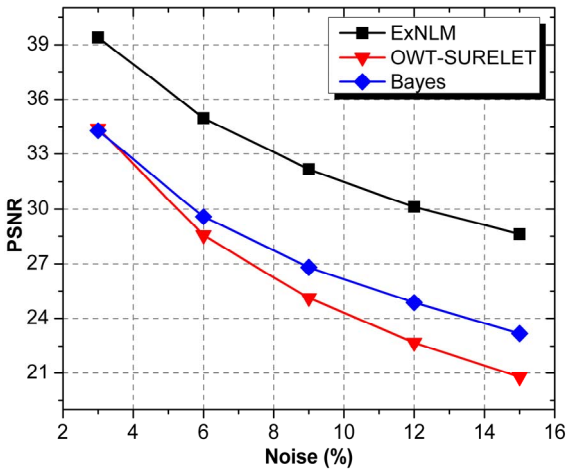

Figure 5: Quantitative comparison of ExNLM with other contemporary methods in terms of PSNR

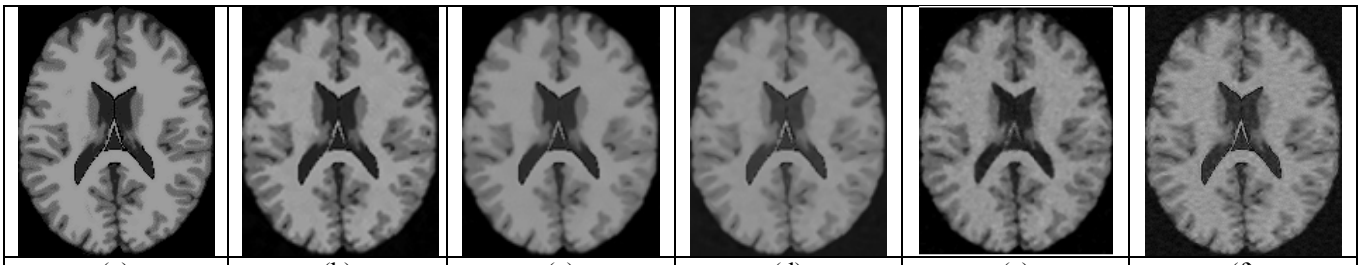

(a)	(b)	(c)	(d)	(e)	(f)

Figure 6, Visual results of several de-noising algorithms, (a) A original brain MR image, corresponding restored image using (b) ExNLM, (c) UNLM, (d) IANLM, (e) Bayes estimation denoising, (f) OWT-SURELET

I. CONCLUSION

Non-local means (NLM) is a patch based image de-noising method which exploits natural structural redundancy in a noisy image to restore higher quality image. In this work, we have extended an improved variant of NLM, called improved adaptive non-local means (IANLM), in several ways, and have validated the proposed algorithm on brain MRI data. In particular, the IANLM algorithm is adapted to Rician noise and a wavelet coefficient mixing procedure is proposed for exploiting information in different sub-bands of over- and under-smoothed images obtained by using IANLM algorithm. The new algorithm, named as extended non-local means (ExNLM), has been optimized for application to brain MRI. Different variants of ExNLM have been validated on simulated brain MR images in order to test the influence of different extensions to IANLM proposed in this work. Quantitative and qualitative results compared with IANLM and other contemporary de-noising methods verify that the proposed algorithm not only suppresses the noise more effectively but also better preserves small image structures.

REFERENCES

[1] Lie´vin, M., Luthon, F., and Keeve, E.: "Entropic estimation of noise for medical volume restoration", Pattern Recognition, 2002, 3, pp. 871-874

[2] Ashburner, J., and Friston, K.J.: "Voxel-based morphometry - the methods", NeuroImage 2000, 11, pp. 805-821

[3] Gilboa, G., Sochen, N., and Zeevi, Y.Y.: "Image Enhancement and Denoising by Complex Diffusion Processes"," IEEE Transactions on Pattern Analysis and Machine Intelligence, 2004, 26, (8), pp. 1020 - 1036

[4] Perona, P., and Malik, J.: "Scale-space and edge detection using anisotropic diffusion", IEEE Transactions on Pattern Analysis and Machine Intelligence, 1990, 12, pp. 629-639

[5] Samsonov, A., and Johnson, C.: "Noise-adaptive nonlinear diffusion filtering of MR images with spatially varying noise levels", Mag. Res. in Med., 2004, 52, pp. 798-806

[6] Luisier, F., Blu, T., and Unser, M.: "A New SURE Approach to Image Denoising: Interscale Orthonormal Wavelet Thresholding", IEEE Transactions on Image Processing, 2007, 16, (3), pp. 593-606

[7] Selesnick, I.W.: "The Double-Density Dual-Tree DWT", IEEE Trans. on Sign. Proc., 2004, 52, (5), pp. 1304-1314

[8] Buades, A., Coll, B., and Morel, J.M.: "A review of image denoising algorithms with a new one", Multiscale Modeling and Simulation, 2005, 4, (2), pp. 490–530

[9] Coupe, P., Yger, P., Prima, S., Hellier, P., Kervrann, C., and Barillot, C.: "An optimized blockwise Nonlocal Means denoising filter for 3-D Magnetic Resonance Images", IEEE Transactions on Medical Imaging, 2008, 27, (4), pp. 425-441

[10] Manjon, J.V., Caballero, J.C., Lull, J.J., Marti, G.G., Bonmati, L.M., and Robles, M.: "MRI denoising using Non-Local Means", Medical Image Analysis, 2008, 12, (4), pp. 514–523

[11] Aksam, I.M., Jalil, A., Rathore, S., Ali, A., and Hussain, M.: "Brain MRI denoizing and segmentation based improved adaptive non-local means", International Journal of Imaging Systems and Technology, article in press, DOI 10.1002/ima.22057, 2013, article in press

[12] Wiest-Daesslé, Prima, S., Coupé, P., Morrissey, S.P., and Barillot, C.: 'Rician noise removal by non-Local Means filtering for low signal-to-noise ratio MRI: applications to DT-MRI', in Editor (Ed.)^(Eds.): 'Book Rician noise removal by non-Local Means filtering for low signal-to-noise ratio MRI: applications to DT-MRI' (2008, edn.), pp. 171-179

[13] Nowak, R.D.: "Wavelet-based Rician noise removal for Magnetic Resonance Imaging", IEEE Transactions on Image Processing, 1999, 8, (10), pp. 1408–1419

[14] Vega, A.T., Perez, V.G., Fernandez, S.A., and Westin, C.F.: "Efficient and robust nonlocal means denoising of MR data based on salient features matching", Computer Methods and Programs in Biomedicine, 2012, 105, (2), pp. 131–144

[15] Coupe, P., Hellier, P., Prima, S., Kervrann, C., and Barillot, C.: "3D Wavelet Subbands Mixing for Image Denoising", International Journal of Biomedical Imaging, 2008, 2008, pp. doi:10.1155/2008/590183

[16] Coupe, P., Manjón, J.V., Robles, M., and Collins, D.L.: "Adaptive Multiresolution Non-Local Means Filter for 3D MR Image Denoising", IET Image Processing, 2012, 6, (5), pp. 558-568

[17] Macovski, A.: "Noise in MRI", Magnatic Resonance in Medicine, 1996, 36, pp. 494–497

[18] Wong, A., Mishra, A., Bizheva, K., and Clausi, D.A.: "General Bayesian estimation for speckle noise reduction in optical coherence tomography retinal imagery", Optics Express, 2010, 18, (8), pp. 8338-8352